



On blob generation mechanisms in tokamak edge plasma

K. Bodi^a, A.I. Smolyakov^b, S.I. Krasheninnikov^{a,*}

^a University of California at San Diego, La Jolla, CA 92093, USA

^b University of Saskatchewan, Saskatoon, S7N5E2, Canada

ARTICLE INFO

PACS:

52.40.Hf

52.25.Vy

52.55.Fa

ABSTRACT

The four-wave interaction technique is used to demonstrate the impact of primary electrostatic (drift wave) turbulence on the generation of large-scale electromagnetic structures (blobs). The analysis includes finite ion temperature effects and the associated diamagnetic contributions to the Reynolds stress. The impact of equilibrium plasma density variation on blob propagation is also discussed.

© 2009 Elsevier B.V. All rights reserved.

1. Introduction

Cross-field plasma transport in both L- and H-mode plasmas is characterized by intermittent radial convection of filamentary structures elongated along the magnetic field (see Ref. [1]). Such coherent meso-scale structures have been called blobs and ELM filaments in L- and H-mode regimes, respectively. While peeling – ballooning instabilities and their subsequent nonlinear saturation have been cited as the mechanism of ELM generation [2], plasma polarization (due to magnetic field curvature) has been suggested (see Ref. [3] and the references therein) to be an underlying mechanism for the formation and convection of blobs. It has also been recently proposed that nonlinear plasma polarization due to Reynolds stresses associated with small-scale drift wave turbulence can be an important factor in the formation of electromagnetic meso-scale structures i.e., blobs [4].

Generically, the process of formation of meso-scale structures as a result of modulational instability of drift waves has been a subject of intensive studies for a long time [5]. It is widely recognized now that such structures, in particular zonal flows, play a critical role in regulation and saturation of drift wave turbulence and transport [6]. Our analysis of turbulent blob generation in [4] was based on the application of the wave kinetic equation approach. Here we consider the same process of blob generation by using the four-wave interaction approach. We also discuss the effects of equilibrium plasma density variation on the propagation of seeded blobs.

In Section 2, we present the system of equations and review the results of Ref. [4]. In Section 3, we consider the generation of blobs through the modulational instability of drift waves based on the four-wave interactions. In Section 4, we discuss the effects of the

equilibrium plasma density variation on the blob propagation and in Section 5 we summarize the results of the paper.

2. Governing equations

We use a system of reduced fluid equations (the notation is standard) that can be obtained from standard fluid equations by expansion in $1/B$ parameter [7]. In the low frequency, $\omega < \omega_{ci}$, and long wavelength, $k_{\perp}^2 \rho_i^2 < 1$ approximations, for low plasma pressure $\nabla \times \vec{B} = 0$, the electron continuity equation reduces to a simple form:

$$\left(\frac{\partial}{\partial t} + \vec{V}_E \cdot \nabla \right) n - 2(n\vec{V}_E + n\vec{V}_{pe} \cdot \nabla \ln B - \frac{1}{e} \nabla_{\parallel} J) = 0. \quad (1)$$

where $\vec{V}_E = (\vec{e}_z \times \nabla \phi)/B$, $\vec{V}_{pe} = -(\vec{e}_z \times \nabla p_e)/(enB)$, and $\vec{e}_z = \vec{b}$ is the direction of the local magnetic field. The nonlinear parallel gradient operator $\nabla_{\parallel}(\dots)$ is defined as

$$\begin{aligned} \nabla_{\parallel}(\dots) &= \partial(\dots)/\partial z + (\vec{B} \cdot \nabla(\dots))/B \\ &= \partial(\dots)/\partial z - (\hat{e}_z \cdot \nabla A \times \nabla(\dots))/B_0 \end{aligned} \quad (2)$$

Here A is the parallel component of the vector potential that describes magnetic perturbations $\vec{B} = -\vec{e}_z \times \nabla A$. The parallel component of the electric current is $J = -(1/\mu_0) \nabla_{\perp}^2 A$. In the regime, $\omega < k_{\parallel} v_{Te}$, which is assumed in our work, Ohm's law is

$$\partial A / \partial t + \nabla_{\parallel}(\phi - (T_e/e) \ln n) = 0 \quad (3)$$

For finite T_i plasma, inertial polarization drift and the ion drift due to gyroviscosity contribute to the Reynolds stress, which is responsible for generation of large-scale structures; hence these terms are retained in the present analysis. Taking into account the gyroviscous cancellation (e.g. see Refs. [7,8]), ion continuity equation is

* Corresponding author. Address: University of California at San Diego, 9500 Gilman Dr., La Jolla, CA 9209, USA.

E-mail address: skrash@mae.ucsd.edu (S.I. Krasheninnikov).

$$\left(\frac{\partial}{\partial t} + \vec{V}_E \cdot \nabla\right) \mathbf{n} - 2(\vec{V}_E + \vec{V}_{pi}) \mathbf{n} \cdot \nabla \ln B - n_0 \rho_i^2 \nabla_{\perp} \cdot \frac{d_0}{dt} \left(\frac{e \nabla_{\perp} \phi}{T_i} + \frac{\nabla_{\perp} p_i}{p_i} \right) = 0 \quad (4)$$

where, $\vec{V}_{pi} = (\vec{e}_z \times \nabla p_i) / (enB)$, $\frac{d_0}{dt} = \frac{\partial}{\partial t} + \left(\frac{1}{B_0}\right) \vec{e}_z \cdot \nabla \phi \times \nabla$. Quasineutrality equation is

$$-\nabla_{\parallel} j + (2/B)(\vec{e}_z \times \nabla(p_e + p_i)) \cdot \nabla \ln B + en_0 \rho_i^2 \nabla_{\perp} \cdot \frac{d_0}{dt} \left(\frac{e \nabla_{\perp} \phi}{T_i} + \frac{\nabla_{\perp} p_i}{p_i} \right) = 0 \quad (5)$$

2.1. Separation of scales

In the following analysis, all perturbed quantities are represented as a sum of large-scale and small-scale components, $X = X_k + X_q$, $q < k$, where k and q are the small and large-scale wave-numbers respectively. An analogous separation of scales is assumed in the time domain, $\Omega_q < \omega_k$: ω_k are the eigen-frequencies of small-scale fluctuations, $X_k(t) \sim \exp(-i\omega_k t)$ and Ω are the large-scale mode frequencies, $X_q(t) \sim \exp(-i\Omega t)$. The latter are affected by nonlinear effects and can deviate significantly from the linear eigenvalues.

2.2. Inverse cascade and ballooning instability of meso-scale structures

In Ref. [4], blob generation was explained as a synergy of the interchange drive and nonlinear effects associated with drift wave turbulence. The Reynolds stress was obtained using the wave kinetic equations. Based on the resulting dispersion relation, an instability criterion was derived for the ensemble averaged magnitude ($\langle \phi \rangle$) and length-scales ($\langle k_x \rangle$) of the fluctuations for the destabilizing turbulent stresses to overcome the Alfvén stabilization (for $\beta = c_s^2/v_A^2$)

$$\rho_s(k_x) e \langle \phi \rangle / T > 1 / (q_s R q_y \sqrt{\beta}), \quad (6)$$

where q_s is the safety factor. For the large-scale modes, an instability criterion was derived to explain the length-scales, Δ , of the meso-scale structures. A simple, order of magnitude estimate was obtained for large plasma fluctuations by taking $q_y \Delta \sim 1$, and neglecting the destabilizing effect of turbulent stresses in the instability criterion

$$c_s^2 / R \Delta - c_s^2 \rho_s^2 / \Delta^4 > V_A^2 / q_s^2 R^2 \quad (7)$$

where q_s is the safety factor. The competition of the first and second terms defines the characteristic size of meso-scale structure for which the left hand side is maximal:

$$\Delta_m \approx (\rho_s^2 R)^{1/3} \quad (8a)$$

(we assume that $\Delta_m < L_n$, where L_n is the density scale length). Then the instability within this flux tube occurs for relatively high beta at the edge of plasma

$$\beta > q_s^{-2} (\rho_s / R)^{2/3}. \quad (8b)$$

2.3. Numerical simulations

In order to verify our analytic estimates we solve 2D version of Eqs. 1, 3, 5, with the assumption that the parallel scale length of the perturbations is $\sim q_s R$. We chose sub-critical gradient of plasma density to seed a large amplitude drift wave (satisfying Eq. (6)). Preliminary results show qualitative agreement with the physical picture of blob generation described above and demonstrate blob

formation and detachment for relatively large amplitude of drift waves (see Fig. 1).

3. Four-wave modulational interactions of drift waves and blob generation

In this section, we follow the approach of four-wave modulational interaction to study blob generation. We proceed from the above-described separation of scales, and for the primary fluctuations, we consider simple drift wave type fluctuations assuming that primary modes are electrostatic and that the condition $\omega < k_{\parallel} v_{Te}$ is satisfied. The ion response takes into account the equilibrium gradients of density and ion temperature (which are assumed to be small enough to avoid ITG instability). In the lowest order, neglecting the dispersion and the gradient of the equilibrium magnetic field, for $V_* = -(T/eB_0)(d \ln(n_0)/dx)$, we obtain the simple electron drift wave primary fluctuations $\omega = \omega_{*k} = k_y V_*$. Nonlinear interaction of these primary fluctuations with large-scale components leads to the excitation of the sidebands of the perturbed quantities, which can be obtained from the respective governing equations. Defining $\eta_i = \partial \ln T_{oi} / \partial \ln n_0$, we assume that the ion temperature sidebands follow the simple relation $T_{\pm k+q} / T_{oi} = \eta_i e \phi_{\pm k+q} / T_e$. This neglects the nonlinear generation of temperature sideband via convection. Since the small-scale fluctuations are electrostatic ($A_k = 0$), Ohm's law can be written as

$$-i(\Omega - q_y V_*) A_{k+q} + i \frac{T_e}{e} (q_z + k_z) \left(\frac{e \phi_{k+q}}{T_e} - \frac{n_{k+q}}{n_0} \right) = 0. \quad (9)$$

Corrections due to A_{k+q} are small (of the dispersive order, e.g. $k_{\perp}^2 \rho_i^2$) and are neglected here. As a result, we have no direct generation of sidebands of the vector potential in the Ohm's law and the sidebands of primary fluctuations remain electrostatic $e \phi_{k+q} / T_e = n_{k+q} / n_0$. Neglecting the dispersive corrections, thus leading to $A_{\pm k+q} = 0$, the large-scale component of the parallel momentum balance remains linear

$$\frac{\partial A_q}{\partial t} + \frac{\partial}{\partial z} \left(\phi_q - \frac{T_e}{e} \frac{\tilde{n}_q}{n_0} \right) + \frac{T_e}{e B_0} \frac{1}{n_0} \vec{e}_z \cdot \nabla A_q \times \nabla n_0 = 0. \quad (10)$$

For $\Omega < q_z v_{Te}$, electron and ion temperature fluctuations are determined by

$$\begin{aligned} \nabla_{\parallel} T_e &= 0 \\ \partial T_{iq} / \partial t + \vec{V}_{Ei} \cdot \nabla T_{oi} &= 0 \end{aligned} \quad (11)$$

Neglecting the magnetic gradient drift and parallel current terms (of the dispersive order) in the electron continuity equation, we have

$$n_q / n_0 = (q V_* / \Omega) e \phi_q / T_e. \quad (12)$$

Denoting the contribution of Reynolds stress as R_1 , the quasineutrality equation is

$$\begin{aligned} \Omega_{Di} \left(\frac{n_q}{n_0} + \frac{T_{iq}}{T_{oi}} \right) - \Omega_{De} \left(\frac{n_q}{n_0} + \frac{T_{eq}}{T_{oe}} \right) - \Omega q_{\perp}^2 \rho_i^2 \left(\frac{n_q}{n_0} + \frac{T_{iq}}{T_{oi}} + \frac{\rho_s^2}{\rho_i^2} \frac{e \phi_q}{T_e} \right) \\ + \frac{q_z q_{\perp}^2}{\mu_0 e n_0} A_q + i \rho_i^2 R_1 = 0, \end{aligned} \quad (13)$$

where $\Omega_{Di,e} = q_y V_{Di,e}$, $V_{Di,e} = \pm 2(T_{i,e} / e B_0) \partial \ln B / \partial x$, $\tau = T_{oi} / T_{oe}$, $\rho_s^2 = T_e / m_i \omega_{ci}^2$.

Linearizing Eq. (11) for the electron and ion temperature fluctuations, and Eq. (12) for density fluctuations, neglecting dispersion in the large-scale components, we obtain the lowest order expressions for the Reynolds stress, leading to the final dispersion relation

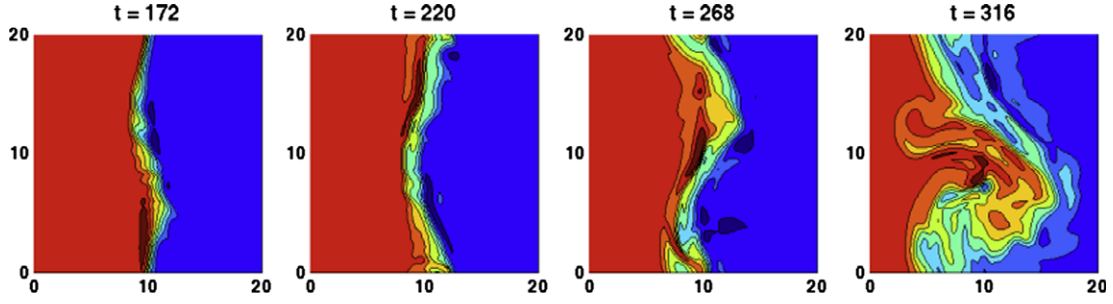


Fig. 1. Evolution of plasma density with seeded drift wave of large amplitude.

$$\begin{aligned} & \Omega^2 + \Omega \Omega_s \tau (1 + \eta_i) - \frac{\Omega_{Di} \Omega_s}{q_\perp^2 \rho_s^2} [1 + \eta_i + \tau^{-1} (1 + \eta_e)] - q_z^2 v_A^2 \\ & = -\frac{2}{B_0^2} |\vec{e}_z \cdot \mathbf{k} \times \mathbf{q}|^2 |\phi_k|^2 (1 + \tau^{-1} + \eta_i) \end{aligned} \quad (14)$$

Here, the second term describes the drift stabilization due to finite ion temperature, the third term is the interchange drive, and the fourth term describes the Alfvén stabilization. The term on the right-hand side is the Reynolds stress drive that takes into account the diamagnetic contributions due to finite ion temperature. Eq. (14) is consistent with results of the previous analysis following the wave kinetic approach [4]. Note that the growth rate of this electromagnetic instability is a factor $q_s \rho_s$ larger than for electrostatic modes with a finite q_y . For a more detailed derivation of the above, we refer the reader to Ref. [9].

4. Blob propagation and plasma density gradient

In this section, we present the results of our numerical study on the behavior of perturbation in electrostatic potential in the presence of a pressure gradient. We consider plasma that is confined in a uniform magnetic field, and normalize the length and time scales with respect to the ion gyro radius and ion cyclotron frequency respectively. We know that a perturbation in the electrostatic potential leads to a local electric field leading to $\vec{E} \times \vec{B}$ drift of this perturbation. Flow relative to this perturbation is two-dimensional and, for slow magnetic field variation, incompressible

($\nabla \cdot \vec{V} = 0$), with a stream-function ϕ : $\vec{V} = \vec{e}_z \times \nabla \phi$, and governed by the Euler equations

$$\frac{\partial}{\partial t} \mathbf{n} + \nabla \cdot (\vec{V}_E \mathbf{n}) = 0 \quad (15)$$

$$\frac{\partial}{\partial t} \Omega + \nabla \cdot (\vec{V} \Omega) + \vec{e}_z \cdot (\nabla \varepsilon \times \nabla \mathbf{n}) = 0 \quad (16)$$

Eq. (16) is the vorticity, $\Omega = \nabla \cdot (\mathbf{n} \nabla \phi)$, equation for non-uniform density where, $\varepsilon = |\nabla \phi|^2 / 2$ is the specific kinetic energy. The energy of such a flow-field is composed only of its kinetic energy in this incompressible limit, $E = \mathbf{n} \varepsilon$, and its evolution can be described as

$$\frac{\partial}{\partial t} E + \nabla \cdot (\vec{V} E) + \nabla \cdot (\vec{V} \mathbf{p}) = 0 \quad (17)$$

We can see that energy is conserved.

For plasma with uniform equilibrium density described by Eq. (15), (16), the blob motion is the same as that of a vortex-pair in an incompressible, irrotational flow. It should be noted that, in the absence of diffusive processes, vorticity is confined to the blob and the flow around the blob remains irrotational. The flow-field relative to the blob can be described by the potential flow theory ($\nabla^2 \phi = 0$). Pressure can be obtained from the energy equation at steady state along a streamline $p + \mathbf{n} v^2 / 2 = \text{const}$. Clearly, such a blob encounters no resultant force along its path. For a flow-field with non-uniform plasma density along the direction of blob

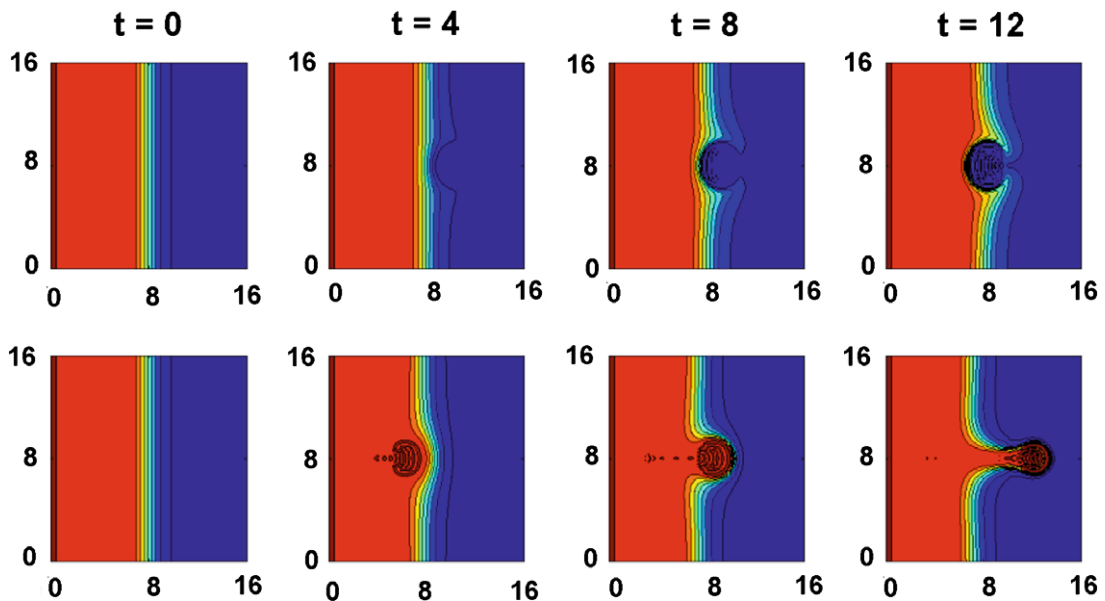


Fig. 2. Density evolution for: a blob moving along increasing density (top) and a blob moving along decreasing density (bottom).

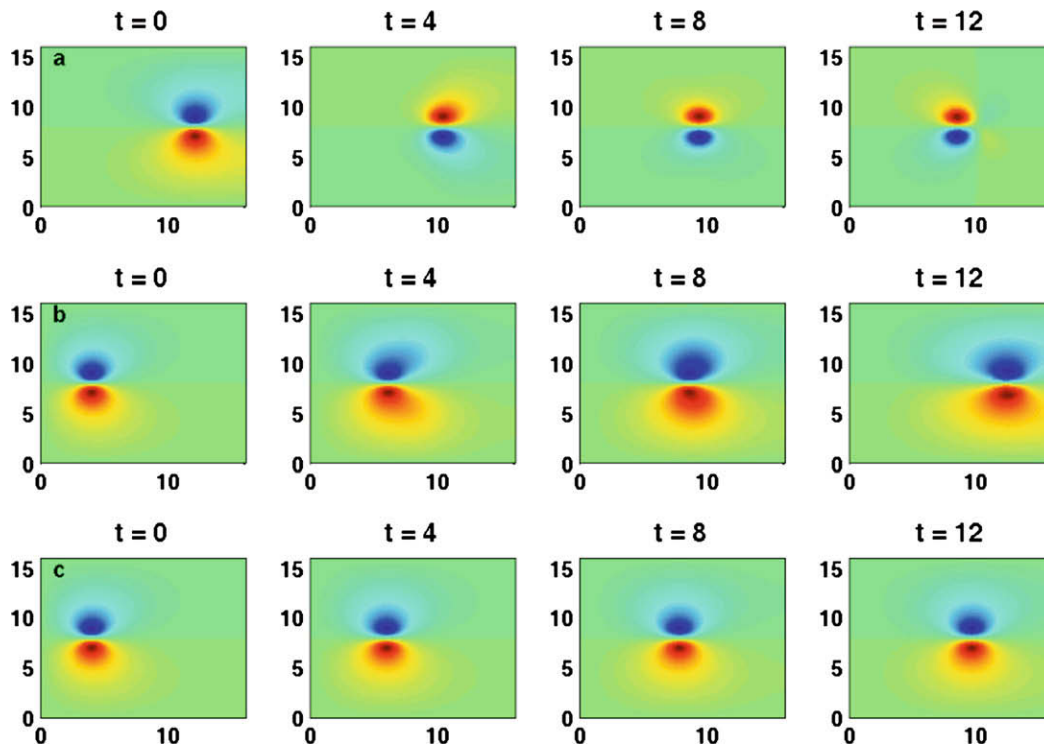


Fig. 3. The contours of electrostatic potential ϕ plots of a blob moving along increasing density (top), a blob moving along decreasing density (middle), and a blob moving through uniform density (bottom).

propagation, though the flow-field is still described by potential flow theory, the surrounding density difference between the leading and trailing faces of the blob leads to a resultant force towards the lower density region. Thus, for non-uniform plasma, perturbations encounter a force against the density gradient.

4.1. Numerical simulations

Computations were carried out to demonstrate the above conclusions. For numerical stability, diffusion and viscosity ($\sim 10^{-3}$)

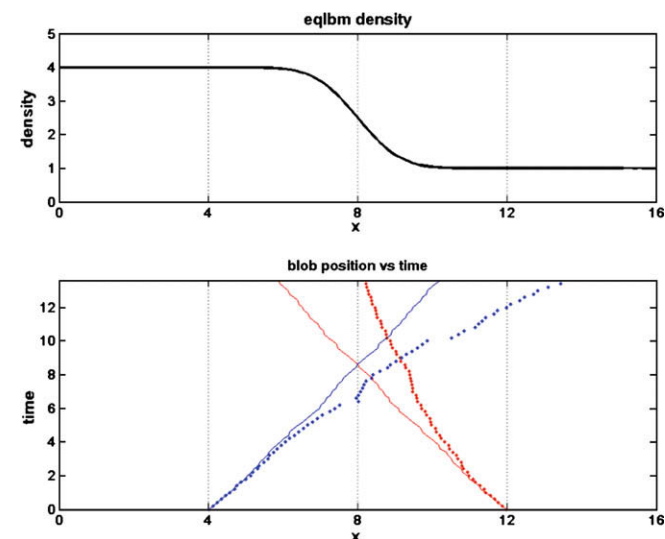


Fig. 4. Top: the equilibrium density profile. Bottom: coordinates of 'center of mass' of the blobs as a function of time a blob initially moving towards increasing density (curve 1) and a blob moving towards decreasing density (curve 2). Dotted lines correspond to inward and outward moving blobs in uniform density plasma.

terms were added to the continuity and the vorticity equations, which were marched in time using third order Runge–Kutta scheme (RKW3). The electrostatic potential ϕ was computed using the following SOR scheme

$$\phi^{n+1} = (1 - \omega) \phi^n + \omega \Delta^{-1} \left(\frac{\Omega}{n} - \frac{1}{n} \nabla n \cdot \nabla \phi \right) \quad (18)$$

with $\omega = 1.2$, and inversion of the Laplacian, Δ^{-1} , was done using a Fourier method. We seed blobs as the perturbations of ϕ ($\max(|\phi|) = 1.0$) in the form of a Gaussian profile and use non-uniform density (see Figs. 2 and 3). Blob position was estimated to be the centroid of ϕ in the region of the domain containing the blob.

It can be seen from Fig. 4 that, for the same time, the outgoing blob traverses a much longer distance compared to the blob propagating in the direction of increasing density where the blob experiences strong deceleration, the blob moving towards decreasing density experiences strong acceleration. Consequently, by the end of the computation, the blob propagating in the direction of decreasing density has reached the boundary, whereas the blob propagating in the direction of increasing density is still in the region of varying density.

5. Conclusions

Using four-wave interaction technique we confirm the results of Ref. [4] that the interplay of the interchange drive and nonlinear effects associated with drift wave turbulence (which is rather strong at the edge in L-mode) can lead to the sub-critical excitation of the interchange mode and blob generation. The impact of equilibrium plasma density variation on the propagation of seeded blobs (no interchange drive) has been studied and clearly demonstrates the preferences for the blobs propagating into low plasma density, suggesting convective nature of non-uniform plasma transport.

Acknowledgements

The work was supported in part by the USDOE grant No. DE-FG02-04ER54739 at UCSD.

References

- [1] D.H.J. Goodall, J. Nucl. Mater. 111&112 (1982) 11;
S.J. Zweben, Phys. Fluids 28 (1985) 974;
J.I. Boedo et al., Phys. Plasmas 8 (2001) 4826;
J.L. Terry et al., J. Nucl. Mater. 290 & 293 (2001) 757;
A. Kirk et al., Plasma Phys. Control. Fus. 48 (2006) B433;
D.L. Rudakov et al., Plasma Phys. Control. Fus. 44 (2002) 717;
A. Kirk et al., Plasma Phys. Control. Fus. 47 (2005) 995.
- [2] J.W. Connor, Plasma Phys. Control. Fus. 40 (1998) 531;
H.R. Wilson, S.C. Cowley, Phys. Rev. Lett. 92 (2004) 175006;
P. Zhu et al., Phys. Plasmas 14 (2007) 055903.
- [3] S.I. Krasheninnikov, Phys. Lett. A 283 (2001) 368;
S.I. Krasheninnikov et al., J. Plasma Phys. published online Jan 2, 2008.
- [4] S.I. Krasheninnikov, A.I. Smolyakov, Phys. Plasmas 14 (2007) 102503.
- [5] R.Z. Sagdeev et al., JETP Lett. 27 (1978) 340;
R.Z. Sagdeev et al., Sov. J. Plasma Phys. 4 (1978) 306;
P.K. Shukla et al., Phys. Rev. A 23 (1981) 31;
J. Weiland et al., Phys. Fluids 24 (1981) 93;
K. Mima, Y.C. Lee, Phys. Fluids 23 (1980) 105.
- [6] A.M. Balk et al., Sov. Phys. JETP 98 (1990) 446;
P.H. Diamond, Y. Kim, Phys. Fluids B 3 (1991) 1626;
V. Naulin, N. J. Phys. 4 (2002) 28;
K. Itoh et al., Phys. Plasmas 13 (2006) 55502;
M.G. Shats, W.M. Solomon, N. J. Phys. 4 (2002) 30;
F. Zonca et al., Phys. Plasmas 11 (2004) 2488;
P.H. Diamond et al., Plasma Phys. Control. Fus. 47 (2005) R35.
- [7] A.B. Mikhailovskii, Theory of Plasma Instabilities, Consultants Bureau, New York, 1974. vol. 2, p. 87.
- [8] M.N. Rosenbluth, A. Simon, Phys. Fluids 8 (1965) 1300;
F.L. Hinton, W. Horton, Phys. Fluids 14 (1971) 116;
A.I. Smolyakov, Can. J. Phys. 76 (1998) 321.
- [9] A.I. Smolyakov, S.I. Krasheninnikov, Phys. Plasmas 15 (2008) 072302.